

Received 00th January 20xx,

High Performance Oxygen-bridged N-shaped Semiconductors with Stabilized Crystal Phase and Blue Luminescence

Chikahiko Mitsui,^a Yuji Tanaka,^b Shota Tanaka,^b Masakazu Yamagishi,^a Katsumasa Nakahara,^c Masafumi Yano,^b Hiroyasu Sato,^d Akihito Yamano,^d Hiroyuki Matsui,^a Jun Takeya,^{a,c} and Toshihiro Okamoto^{*a,c,e}

Accepted 00th January 20xx

DOI: 10.1039/x0xx00000x

www.rsc.org/

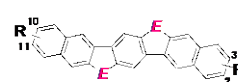
Here, we describe an oxygen-bridged N-shaped π -electron core, dinaphtho[2,3-*d*:2',3'-*d'*]benzo[1,2-*b*:4,5-*b'*]difuran (DNBDF), as a new entity of organic semiconducting materials. Interestingly, by introduction of flexible alkyl chains at appropriate positions, DNBDF π -cores exhibit solution processability, a highly stabilized crystal phase, high mobility, and blue luminescent in solid.

π -electron systems composed of benzene- and/or heterole-fused π -electronic cores, especially, play an indispensable role in driving organic field-effect transistors (OFETs).¹ For the creation of printed devices applicable to displays and radio frequency identifier (RFID) tags,² the development of high performance organic semiconductors for OFETs is a crucial issue. In this context, a large number of promising materials with carrier mobility greater than that of amorphous silicon (0.5–1.0 cm²/Vs) were reported and investigated.³ One of the most important advantages of OFETs to be considered is their solution processability, allowing low-cost device fabrication. However, there is no straightforward way to develop practically applicable organic semiconductors featuring solution processability and a thermally stable aggregate form toward the device thermal durability, because they often result in trade-off relationships.⁴ To overcome this formidable challenge, we newly developed bent-shaped π -electronic cores with oxygen- and sulfur-bridged V-shaped π -conjugated molecules, dinaphtho[2,3-*b*:2',3'-*d'*]chalcogenophene (DNF-V and DNT-V, see Figure 1a).⁵ Indeed, sulfur-bridged derivatives (DNT-Vs) exhibit carrier mobility as high as 9.5 cm²/Vs, and a good device durability under thermal stress up to 150 °C.^{5a}

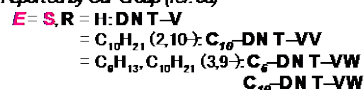
a) V-Shaped π -Core



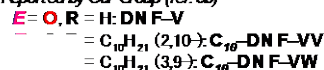
b) N-Shaped π -Core



Reported by Our Group (ref. 5a)



Reported by Our Group (ref. 5b)



Reported by Our Group (ref. 6)

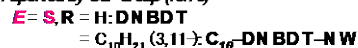
**THIS WORK**

Figure 1. Chemical structures of V- and N-shaped π -cores.

Moreover, we designed sulfur-bridged N-shaped molecules for the π -electron expansion (see Figure 1b). Owing to their extended π -electron conjugation and zig-zag shaped core structure, we successfully demonstrated that **C₁₀-DNBDT-NW** exhibits excellent carrier mobility up to 16 cm²/Vs in solution-crystallized thin film. This OFET proved to be extremely robust against thermal stress, even at 200 °C.⁶ In this work, we focus on the oxygen-bridged N-shaped congeners, dinaphtho[2,3-*d*:2',3'-*d'*]benzo[1,2-*b*:4,5-*b'*]difuran (DNBDF) derivatives, and elucidate their photophysical and thermal properties, aggregated structures and carrier transporting abilities. Notably, the incorporated chalcogen atoms have a significant impact on the electronic properties and aggregate structures, so that the emissive characteristic, thermal stabilities, as well as carrier transporting abilities are quite different among these molecules. Especially, by virtue of the light oxygen atom, previously developed DNF-Vs exhibit deep blue-emission with a high quantum yield in solid state, whereas the sulfur-containing congener, DNT-V, shows almost no emission. Such a high luminescence characteristic could be an additional fascinating feature toward the application of organic light-emitting transistors (OLETs).⁷ In this paper, we describe the syntheses of decyl groups substituted compounds on different positions (on 2 and 10 positions: **C₁₀-DNBDF-NV**; on 3 and 11

^a Department of Advanced Materials Science, School of Frontier Sciences, The Univ. of Tokyo, 5-1-5 Kashiwanoha, Kashiwa, Chiba 277-8561, Japan.

^b Faculty of Chemistry, Materials and Bioengineering, Kansai Univ., 3-3-35 Yamate-cho, Suita, Osaka 564-8680, Japan.

^c The Institute of Scientific and Industrial Research (ISIR), Osaka University, 8-1 Mihogaoka, Ibaraki, Osaka 567-0047, Japan.

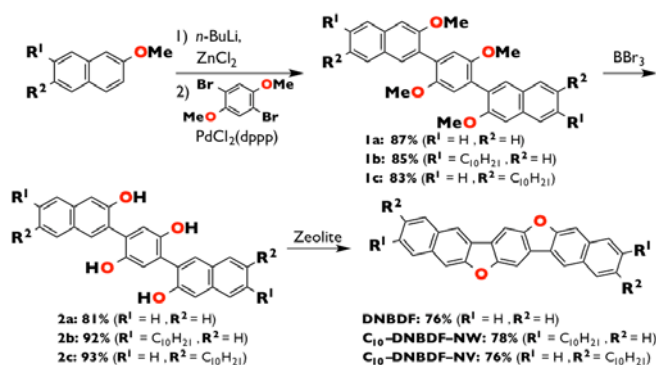
^d Rigaku Corporation, 3-9-12 Matsubara-cho, Akishima, Tokyo 196-8666, Japan.

^e JST, PRESTO, 4-1-8 Honcho, Kawaguchi, Saitama 332-0012, Japan.

† Electronic Supplementary Information (ESI) available: [details of any supplementary information available should be included here]. See DOI: 10.1039/x0xx00000x

positions: **C**₁₀-**DNBDF**-**NW**, Figure 1b) together with the parent

Scheme 1. Synthesis of **DNBDF** Derivatives



DNBDF and the effects of substitution position on their thermal stability, solubility, photophysical properties, and carrier mobility in thin film. Throughout this study, **C**₁₀-**DNBDF**-**NV** exhibits a highly stabilized crystal phase up to 295 °C, blue emission with a moderately high quantum yield of 42%, even with flexible long alkyl chains in solid state, and high carrier mobility up to 1.8 cm²/Vs in solution-crystallized FET, by taking advantage of its moderate solubility. This carrier mobility, determined by FETs, is considerably high among the hitherto developed furan containing materials.⁸

All of the **DNBDF** derivatives were synthesized by utilizing the synthetic protocol, developed by our own as illustrated in Scheme 1. Selective deprotonation of 2-methoxynaphthalene derivatives at the 3-positions, using *n*-BuLi, followed by transmetalation from lithium to zinc and Negishi cross-coupling with 1,4-dibromo-2,5-dimethoxybenzene in the presence of palladium catalyst afforded the coupling compounds **1a–c** in high yields. Subsequent demethylation by boron tribromide gave the target precursors **2a–c**. Finally, by use of a zeolite catalyst,^{5b,9} the dehydration smoothly proceeded producing the target compounds, which were finally purified by multiple recrystallization and vacuum sublimation. The synthesized **DNBDF** derivatives are pale green in solid state, indicating the extension of the π -electron system, in comparison with the colorless **DNF–V** derivatives. Indeed, absorption spectrum measurements clarified that the absorption edge of **DNBDF** in vacuum deposited thin film is 430 nm, which means a bathochromic shift by *c.a.* 20 nm compared with **DNF–V** (see Figure S1). Owing to the π -electron expansion, the ionization potential (IP) value of **DNBDF** in vacuum deposited thin film on ITO, determined by photoelectron yield spectroscopy (PYS) measurements,¹⁰ is 5.70 eV, which is indeed smaller than that of **DNF–V** (5.93 eV). By introduction of alkyl chains in the **DNBDF** core, **C**₁₀-**DNBDF**-**NW** and **C**₁₀-**DNBDF**-**NV** exhibited smaller IP values of 5.67 eV and 5.65 eV, respectively, caused by their electron donating nature (see Figure S4).

We have studied the photophysical and thermal properties of **DNBDF** derivatives. The emission characteristics were investigated in both solution and solid. In solution, all three molecules exhibit blue emission with a high quantum yield of 65–78%. Even in solid, **DNBDF** itself shows a high quantum yield of 71%. **C**₁₀-**DNBDF**-**NW** and **C**₁₀-**DNBDF**-**NV** show lower but moderate quantum yields of 42% and 36% due to the existence of flexible alkyl chains, respectively. Thermogravimetric analysis (TGA) showed the higher weight loss

temperature (see Figure S5). By heating the samples under a nitrogen gas atmosphere, the 5% weight loss temperatures (*T*^{95%}) were determined to be 365 °C for **DNBDF**, 434 °C for **C**₁₀-**DNBDF**-**NW**, and 420 °C for **C**₁₀-**DNBDF**-**NV**, respectively. In contrast, V-shaped congeners, **DNF–V**, **C**₁₀-**DNF**-**VW**, and **C**₁₀-**DNF**-**VV** start to evaporate at lower temperatures with a *T*^{95%} of 268 °C, 359 °C, and 365 °C. The higher weight loss temperatures of **DNBDF** derivatives are ascribed to their large molecular weight as well as the stronger dispersion energy between extended **DNBDF** π -cores. A remarkable substitution effect was observed in the stabilized crystal phase and solubility. Phase-transition temperatures of alkylated **DNBDF**s were also measured by differential scanning calorimetry (DSC). It is noteworthy that the phase-transition temperature from the crystal phase of **C**₁₀-**DNBDF**-**NW** is just 104 °C, whereas that of **C**₁₀-**DNBDF**-**NV** is significantly higher (295 °C) (see Figure S6). In comparison, the smaller V-shaped π -core derivatives, **C**₁₀-**DNF**-**VW** and **C**₁₀-**DNF**-**VV**, show phase-transition at 128 °C and 176 °C, respectively. Thus, the substitution at the 2,10 positions of the **DNBDF** core endows them with a thermally stabilized crystal phase. A solubility test was performed for these three compounds to choose the appropriate material for the fabrication of solution processed FETs. Although unsubstituted **DNBDF** is insoluble in 1,2,4-trichlorobenzene at 90 °C (less than 0.01 wt%), alkylated ones possess 0.037 wt% for **C**₁₀-**DNBDF**-**NW** and 0.16 wt% for **C**₁₀-**DNBDF**-**NV** in the same condition, respectively. These results suggest that both alkylated **DNBDF** compounds possess solution processability at slightly high temperature.

In order to clarify the aggregate structures for understanding the carrier-transporting ability by using theoretical calculations, X-ray single crystal analyses were performed. All single crystals, grown by either horizontal physical vapour transport^{11,12} or solution crystallization technique by gradient cooling, show platelet forms. X-ray structural analyses revealed that all **DNBDF** derivatives stack into a two-dimensional herringbone packing structure regardless of the presence and position of alkyl side chains (Figure 2). For all **DNBDF**s, C–H short contacts were observed between the neighboring molecules attracted with the CH/ π interaction, which could play the role of organizing the herringbone structures. This trend is quite different from the sulfur-bridged case. Actually, the **DNBDT** forms a slipped π - π stacking structure and thus exhibits a poor carrier mobility of 0.03–0.06 cm²/Vs in single crystal FETs. Meanwhile, **C**₁₀-**DNBDT**-**NW**, forming a two-dimensional herringbone packing structure, shows carrier mobility as high as 16 cm²/Vs.⁶ (Note: **C**₁₀-**DNBDT**-**NV** forms a different packing structure. The details on the packing structures and its carrier transporting ability will be reported elsewhere.) We conjectured that the sterically less demanding oxygen atom and thus the larger obtuse angle of the **DNBDF** core enable all types of **DNBDF** derivatives to interact each other by CH/ π interaction and thus form herringbone packing structures, which are favourable for a two-dimensional carrier transport. To quantitatively analyse their carrier transporting ability, band structure calculations were conducted based on the packing structure by way of periodic boundary condition at the PBEPBE/6-31G(d) level (see Figure S8–11). In band structures of **DNBDF**s, large band dispersion at the top of the valence band is observed in both directions in the conduction plane, indicating the potential of two-dimensional carrier transport. The calculated hole effective masses are inserted in Figure 2.

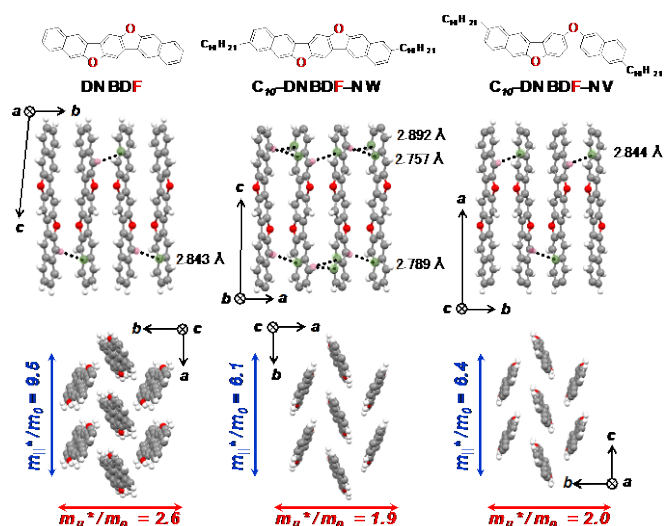


Figure 2. Single crystal structures and effective masses of DNBDf derivatives.

The effective mass is inversely proportional to carrier mobility as described by the following equation; $\mu = q\tau/m^*$ (μ : mobility, q : carrier charge, τ : relaxation time, m^* : effective mass).¹³ Both alkylated DNBDfs possess almost the same hole effective masses as those of C_{10} -DNBDf-VW. Notably, they possess anisotropic values; that is, the effective masses in the transverse direction (m_{\perp}^*) are much smaller than those in the columnar direction (m_{\parallel}^*) (Figure 2). In contrast, unsubstituted DNBDf possesses larger effective masses, in both the columnar and transverse directions, than those of alkylated ones. We assume this is due to the unsubstituted DNBDf standing with a slightly tilted angle on a - b plane, the conduction plane. Thus, the introduction of a long alkyl side chain can finely tune the packing structures. Throughout the comprehensive investigation in terms of a stabilized crystal phase, solution processability, and carrier transporting capability, C_{10} -DNBDf-NV proves to be the best candidate as solution-processable OFET material in this study.

Finally, to clarify the carrier transporting capability, we fabricated OFETs with C_{10} -DNBDf-NV in form of single-crystalline films prepared by *edge-casting*, a solution-crystallization method originally developed by our group.¹⁴ A droplet of a 0.05 wt% hot solution of C_{10} -DNBDf-NV in 1,2,4-trichlorobenzene at 120 °C was placed at the edge of a liquid-sustaining piece on a SiO₂ substrate preliminarily treated with β -phenylethyltrichlorosilane (β -PTS).¹⁵ Along the direction of the solvent-evaporation at a substrate temperature of 90 °C, a large-domain crystalline film formed on the substrate. On top of the prepared single-crystalline film, we made the contacts through a shadow mask to construct the channel in parallel to the crystal growth direction. Thus, FET was fabricated by successive deposition of F₄-TCNQ and the Au electrodes to construct the bottom-gate-top-contact architecture. The electron-accepting F₄-TCNQ layer facilitates hole injection from the gold electrode.¹⁶ The FET of C_{10} -DNBDf-NV operates as a p -type transistor with hole mobility up to 1.8 cm²/Vs (1.3 cm²/Vs in average among 10 devices; see Figure S13–17) and a threshold voltage of –90 V (Figure 3). The

molecular orientation and morphology of the obtained crystalline thin films were investigated by means of X-ray diffraction (XRD). The in-plane and out-of-plane XRD data for C_{10} -DNBDf-NV revealed that the a -axis was oriented perpendicular to the substrate, and the b - c plane was parallel to the substrate, which the film structure of C_{10} -DNBDf-NV is desirable to 2D charge transporting (see Figure S18). Importantly, as the band calculation reveals, the crystal growth direction corresponds to the c axis direction, in which this material shows a larger effective mass ($m_{\parallel}^*/m_0 = 6.4$) compared to the b axis direction ($m_{\perp}^*/m_0 = 2.0$). However, in vertical to the highly conductive b axis direction, some occasional cracks appear in the solution-crystallized film (see Figure S19). Therefore, to demonstrate the intrinsic carrier mobility, it is necessary to measure the FET in the b -direction after optimizing the crystal growth condition to avoid cracks.

In summary, we designed and synthesized DNBDfs, oxygen-bridged N-shaped materials for the application in OFETs. In comparison with DNBDf-V derivatives, DNBDfs possess a smaller ionization potential and a higher weight loss temperature due to the π -extension. Notably, C_{10} -DNBDf-NV exhibits a considerably high phase-transition temperature of 295 °C and a moderately high

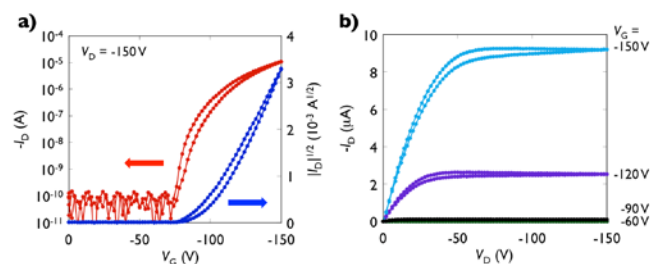


Figure 3. a) Transfer characteristics and b) output characteristics of the typical transistor with the solution-crystallized C_{10} -DNBDf-NV film.

photoluminescent quantum yield of 42% in solid state. Single crystal analyses revealed that all DNBDfs synthesized in this study show a herringbone packing structure. Solution crystallized thin film transistors using C_{10} -DNBDf-NV show high hole mobility of up to 1.8 cm²/Vs. There is room to elevate the carrier mobility of this material by further optimizing the film growth process. Device thermal durability tests and applications of these materials in light-emitting devices are currently underway in our laboratory.

Notes and references

The authors thank Dr. T. Suzuki and Mr. T. Takehara for the XRD measurement of C_{10} -DNBDf-NV in solution-crystallized thin film. C.M. thanks the JSPS Grant-in-Aid for Young Scientists (B) (No.25810118). M. Y. thanks the JSPS Grant-in-Aid for Scientific Research (C) (No. 26410254) and the Kansai University Subsidy for Supporting Young Scholars, 2014. T.O. also thanks the JSPS Grant-in-Aid for Scientific Research (B) (No.25288091). The authors thank the Comprehensive Analysis Center (CAC), ISIR, Osaka University for the measurement of the elemental analysis. This work was financially supported by JNC Petrochemical Corp. and JNC Corp., JAPAN.

- 1 Z. Bao and J. Locklin, *Organic Field-Effect Transistors*, 1st ed.; CRC Press: Florida, 2007.
- 2 (a) P. F. Baude, D. A. Ender, M. A. Haase, T. W. Kelley, D. V. Muyres and S. D. Theiss, *Appl. Phys. Lett.*, 2003, **82**, 3964; (b) S. Steudel, K. Myny, V. Arkhipov, C. Deibel, S. De Vusser, J. Genoe and P. Heremans, *Nat. Mater.*, 2005, **4**, 597.
- 3 (a) J. E. Anthony, *Chem. Rev.*, 2006, **106**, 5028; (b) C. Wang, H. Dong, W. Hu, Y. Liu and D. Zhu, *Chem. Rev.*, 2011, **112**, 2208.
- 4 (a) J. Chen, J. Anthony and D. C. Martin, *J. Phys. Chem. B*, 2006, **110**, 16397; (b) H. Ebata, T. Izawa, E. Miyazaki, K. Takimiya, M. Ikeda, H. Kuwabara and T. Yui, *J. Am. Chem. Soc.*, 2007, **129**, 15732.
- 5 (a) T. Okamoto, C. Mitsui, M. Yamagishi, K. Nakahara, J. Soeda, Y. Hirose, K. Miwa, H. Sato, A. Yamano, T. Matsushita, T. Uemura and J. Takeya, *Adv. Mater.*, 2013, **25**, 6392; (b) K. Nakahara, C. Mitsui, T. Okamoto, M. Yamagishi, H. Matsui, T. Ueno, Y. Tanaka, M. Yano, T. Matsushita, J. Soeda, Y. Hirose, H. Sato, A. Yamano and J. Takeya, *Chem. Commun.*, 2014, **50**, 5342.
- 6 C. Mitsui, T. Okamoto, M. Yamagishi, J. Tsurumi, K. Yoshimoto, K. Nakahara, J. Soeda, Y. Hirose, H. Sato, A. Yamano, T. Uemura and J. Takeya, *Adv. Mater.*, 2014, **26**, 4546.
- 7 F. Cicoira and C. Santato, *Adv. Funct. Mater.*, 2007, **17**, 3421.
- 8 (a) O. Gidron and M. Bendikov, *Angew. Chem. Inter. Ed.*, 2014, **53**, 2546; (b) M. Watanabe, W.-T. Su, Y. J. Chang, T.-H. Chao, Y.-S. Wen and T. J. Chow, *Chem. Asian J.*, 2013, **8**, 60; (c) K. Oniwa, T. Kanagasekaran, T. Jin, M. Akhtaruzzaman, Y. Yamamoto, H. Tamura, I. Hamada, H. Shimotani, N. Asao, S. Ikeda and K. Tanigaki, *J. Mater. Chem. C*, 2013, **1**, 4163; (d) O. Gidron, A. Dadvand, E. Wei-Hsin Sun, I. Chung, L. J. W. Shimon, M. Bendikov and D. F. Perepichka, *J. Mater. Chem. C*, 2013, **1**, 4358; (e) K. Niimi, H. Mori, E. Miyazaki, I. Osaka, H. Kakizoe, K. Takimiya and C. Adachi, *Chem. Commun.*, 2012, **48**, 5892; (f) C. Mitsui, J. Soeda, K. Miwa, H. Tsuji, J. Takeya and E. Nakamura, *J. Am. Chem. Soc.*, 2012, **134**, 5448; (g) M. Nakano, H. Mori, S. Shinamura and K. Takimiya, *Chem. Mater.*, 2011, **24**, 190; (h) O. Gidron, A. Dadvand, Y. Sheynin, M. Bendikov and D. F. Perepichka, *Chem. Commun.*, 2011, **47**, 1976; (i) Y. Miyata, M. Terayama, T. Minari, T. Nishinaga, T. Nemoto, S. Isoda and K. Komatsu, *Chem. Asian J.*, 2007, **2**, 1492.
- 9 A. Arienti, F. Bigi, R. Maggi, P. Moggi, M. Rastelli, G. Sartori and A. Trere, *J. Chem. Soc., Perkin Trans. 1*, 1997, 1391.
- 10 M. Honda, K. Kanai, K. Komatsu, Y. Ouchi, H. Ishii and K. Seki, *Mol. Cryst. Liq. Cryst.*, 2006, **455**, 219.
- 11 R. A. Laudise, C. Kloc, P. G. Simpkins and T. Siegrist, *J. Cryst. Growth*, 1998, **187**, 449.
- 12 For preparation of single crystals of **DNBDF**, horizontal physical vapor transport technique was applied. The length and diameter of Pyrex tube used are 120 cm and 2 cm, respectively. Under Ar carrier gas flow as a flow rate of 50 ccm, source and crystallization-zone temperature were maintained at 350 °C and 260 °C, respectively.
- 13 M. C. R. Delgado, E.-G. Kim, D. A. d. S. Filho and J.-L. Bredas, *J. Am. Chem. Soc.*, 2010, **132**, 3375.
- 14 T. Uemura, Y. Hirose, M. Uno, K. Takimiya and J. Takeya, *Appl. Phys. Exp.*, 2009, **2**, 111501.
- 15 T. Umeda, D. Kumaki and S. Tokito, *J. Appl. Phys.*, 2009, **105**, 024516.
- 16 T. Minari, T. Miyadera, K. Tsukagoshi, Y. Aoyagi and H. Ito, *Appl. Phys. Lett.*, 2007, **91**, 053508.